Journal of Macromolecular Science, Part A
Publication details, including instructions for authors and subscription information:
http://www.informaworld.com/smpp/title~content=t713597274

The Interrelation Between the Microphase Structure of Sequential Interpenetrating Polymer Networks and the Crosslinking Density of Penetrating Networks

V. V. Shilov[a]; S. Yu. Lipatov[a]; Yu. P. Gomza[a]; E. I. Oranskaya[a]; V. F. Matyushov[a]
[a] The Institute of Macromolecular Chemistry Academy of Sciences Ukrainian SSR, Kiev, USSR

To cite this Article Shilov, V. V. , Lipatov, S. Yu. , Gomza, Yu. P. , Oranskaya, E. I. and Matyushov, V. F.(1990) 'The Interrelation Between the Microphase Structure of Sequential Interpenetrating Polymer Networks and the Crosslinking Density of Penetrating Networks', Journal of Macromolecular Science, Part A, 27: 4, 459 — 477
To link to this Article: DOI: 10.1080/00222339009349569
URL: http://dx.doi.org/10.1080/00222339009349569

J. MACROMOL. SCI.—CHEM., A27(4), pp. 459–477 (1990)

THE INTERRELATION BETWEEN THE MICROPHASE STRUCTURE OF SEQUENTIAL INTERPENETRATING POLYMER NETWORKS AND THE CROSSLINKING DENSITY OF PENETRATING NETWORKS

V. V. SHILOV, S. YU. LIPATOV, YU. P. GOMZA, E. I. ORANSKAYA, and V. F. MATYUSHOV

The Institute of Macromolecular Chemistry
Academy of Sciences
Ukrainian SSR, 252160, Kiev, USSR

ABSTRACT

The microphase structure of single polyurethane (PU) and acrylate networks as well as sequential interpenetrating polymer networks (IPNs), produced by the forming of a PU network in the presence of monomers of a penetrating network, was studied by small- and wide-angle x-ray analysis. It was established that each network component was of a two-phase structure consisting of disordered phase-separated microregions. The higher crosslink density of the acrylate network results in its higher heterogeneity. In IPNs, phase separation of a complex nature is realized: the PU matrix preserves some features of a single network structure, and the second component forms microregions 5–10 nm in size while retaining a certain level of interpenetration of both network components. The microphase structure parameters of such systems are greatly dependent on the crosslink density of the penetrating network. This suggests the influence of a three-dimensional network of chemical bonds on the interdiffusion of branched fragments of the penetrating network and molecular chains of the matrix, one leading to the retardation of phase separation.

INTRODUCTION

Interpenetrating polymer networks (IPNs) are widely used in various modern technologies. Presently they are one of the most promising and universal adhesives for new composite materials [1–5]. These complex systems are capable of realizing a wide spectrum of physicochemical properties which depend on the extent of component compatibility. The compatibility of IPNs components is determined not only by thermodynamic equilibrium but it can also be controlled by the retardation of phase separation processes in a forming network over a wide range. A major factor is the superposition of topological restrictions on the interdiffusion of segments of one network and fragments of the other [4, 5]. As a result, phase separation is stopped at an intermediate stage of this process, and a heterogeneous structure consisting of stable nonequilibrium, "diffused" phase-separated microregions [6] is formed.

The principles of IPNs formation are the same in the majority of cases, but the details of their realization can be much different, and quite a number of aspects remain vague. In particular, of considerable interest are the relationships between such characteristics of microphase structure as size, shape, and distribution of heterogeneous microregions in bulk, the extent of their approach to equilibrium composition, and other factors of IPNs formation.

These relationships are necessary in order to control the heterogeneity level and, therefore, the properties of such systems. The objective of the present work is to establish the relationship between the sequential IPNs microphase structure and the crosslink density of the penetrating network during polymerization of the matrix network in the presence of penetrating monomers. In fact, the same PU/PMMA systems have recently been studied by several authors by electron microscopy and other methods [7–19]. However, up to now there are few data on the IPNs structure obtained by a combination of small- and wide-angle x-rays.

EXPERIMENTAL

Materials

Polymer materials based on polytetramethylene glycol (PTMG), toluene diisocyanate (TDI), trimethylol propane (TMP), methyl methacrylate (MMA), and ethylene glycol dimethacrylate (EGDM) were the objects of investigation.

PTMG was dried at 373 K under vacuum at 1.33 GPa to a moisture content below 0.03%. TMP was dried under vacuum at the same pressure to a moisture content below 0.05%. TDI (a mixture of 2,4 and 2,6 isomers) was purified by

vacuum distillation. EGDM was passed through a column with freshly prepared aluminum oxide. Inhibitor-purified and dried MMA was double-distilled.

From TDI and TMP (molar ratio 3:1) an adduct was synthesized. The adduct and other components of IPNs were mixed at room temperature with 0.005% dibutyltin diaurate and 0.01% azonitrile butyrate. Then the reaction mixture was evacuated, poured into glass molds, and exposed to room temperature until a polyurethane (PU) matrix was formed. The reaction was essentially complete as indicated by the disappearance of the absorption band of isocyanate groups (2270 cm^{-1}). Thus, the PU network was produced in the presence of monomers of the penetrating network, which was a good solvent. At the next stage the remaining unreacted components (MMA and EGDM) were thermally polymerized at 393 K for 3 h in the presence of the PU matrix.

Single networks were synthesized under the same conditions as the corresponding networks within IPNs. The compositions of the samples are given in Table 1.

Methods

The structures of single networks and IPNs were studied by wide- and small-angle x-ray analysis. Wide-angle studies were performed on a DRON-2.0 diffractometer with nickel-filtered copper anode radiation. The data were recorded by automatic step-by-step scanning of a detector (scintillation counter) in a range of angles from 3 to 40° with steps of 0.2°. Small-angle studies were performed with a Kratky camera [20] according to a standard procedure [21]. To ensure the necessary statistical accuracy of the pulse count, the total range of scattering

TABLE 1. Sample Compositions (wt%)

		Component				
Sample	Sample no.	TDI	PTMG	TPM	MMA	EGDM
Single polymer networks	1	14.3	82	3.7	—	—
	2	—	—	—	97.5	2.5
	3	—	—	—	85	15
	4	—	—	—	50	50
IPNs	5	8.6	49.2	2.2	39	1
	6	8.6	49.2	2.2	35	5
	7	8.6	49.2	2.2	20	20

angles was divided into three regions, and the data were recorded in each region with an optimum slit width of the detector.

The x-ray data were corrected for background scattering and sample thickness [21]. To reduce the small-angle scattering data to absolute units, a Lupolen sample from Prof. Kratky's laboratory was used [22].

A further treatment of the data was performed in the following way. The additive wide-angle and small-angle scattering curves for the compositions were calculated by using the reduced scattering curves for single networks and their volume fractions in IPNs. These curves were compared with the experimental scattering curves for the systems investigated. Some parameters of heterogeneous structure of the systems (mean-square electron density fluctuation (η^2), correlation function $\gamma(r)$, size distribution function for heterogeneous microregions $D_n(d)$) were calculated according to the FFSAXS program [23].

RESULTS AND DISCUSSION

Single Network Components

Wide-angle curves for single polymer networks as components of IPNs are given in Fig. 1. On the scattering curve for the PU network, one intense, diffuse maximum with a peak near 20° is observed. Such wide-angle scattering profiles are typical of liquid and amorphous flexible-chain polymers. They point to an exclusive short-range order in molecular chain fragments without any elements of long-range order [21, 24].

The scattering curves for MMA networks with different crosslink densities are also of diffuse character, reflecting an amorphous structure. Two maxima are observed for each curve. At a minimum crosslink density (lowest EGDM content), the wide-angle curve for the acrylate network is similar to the scattering curve for linear poly(methyl methacrylate) [25], but with a growing crosslink density, the wide-angle diffraction profile is changed. The quantitative data on positions, heights, and half-widths of wide-angle maxima for polymer networks are given in Table 2. It follows that the wide-angle maxima for the PU and acrylate networks appear at considerably different angles. With an EGDM content increase, the half-widths of both maxima for the acrylate networks grow, the intensity of these maxima falls, and the first one is shifted to wider angles. The changing profile of the first maximum can be associated with the distortion of short-range order of the molecular chain fragments inherent in poly(methyl methacrylate). Such distortion is due to the implantation of four-functional EGDM units. The corresponding changes of the second maximum are connected with the redistribution of intrachain distances due to structural changes of the molecular chains.

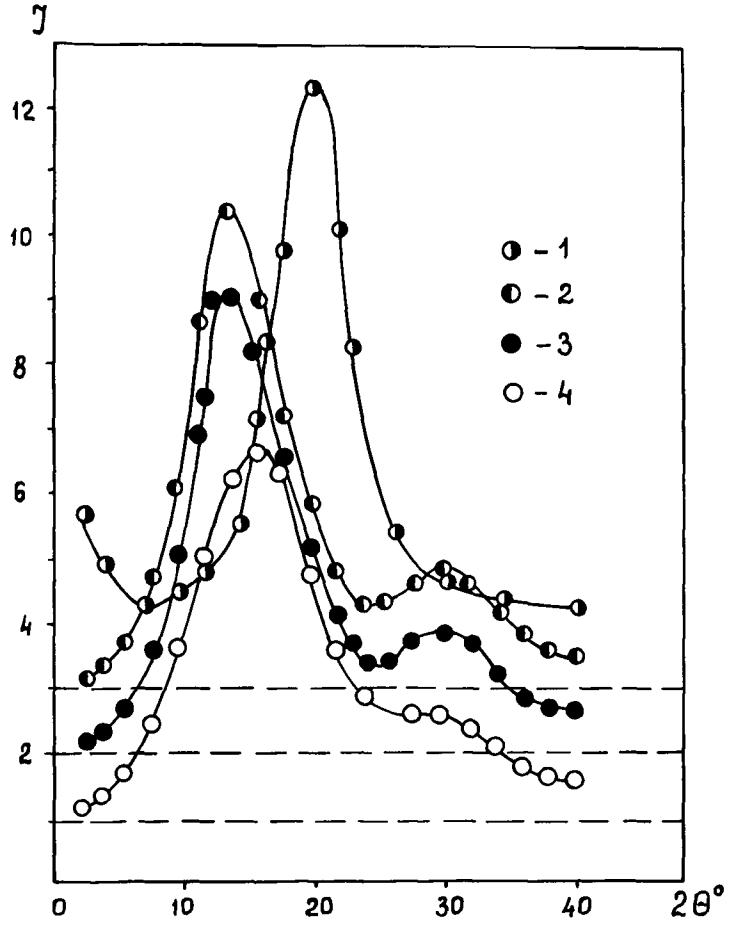

FIG. 1. Wide-angle scattering curves for single polymer networks. In this and the following figures, the curve numbers correspond to the sample numbers in Table 1.

TABLE 2. Characteristics of Wide-Angle Diffraction Maxima for Single Polymer Networks

	Maximum					
	First			Second		
Sample no.	Position, degrees	Height, arbitrary unit	Half-width, degrees	Position, degrees	Height, arbitrary unit	Half-width, degrees
1	20.1	9.4	6.4	—	—	—
2	16.5	8.4	7.7	29	2.0	6.2
3	15.8	8.0	8.2	30	1.8	6.4
4	11.7	6.7	9.3	31	0.7	7.0

After desmearing, small-angle scattering curves for single polymer networks were plotted in absolute units (Fig. 2). Note that the scattering intensity of the PU network is much higher than that of the acrylate network. This can be explained in the following way. The PU network is of polyblock structure, i.e., its molecular chains consist of a sequence of soft glycol and hard urethane blocks. The incompatibility of such blocks usually results in microregions enriched with one of the above-mentioned species. This phenomenon, typical of linear and network block copolyurethane [5, 26], causes microphase separation. But as opposed to the majority of similar systems, our polyurethane sample is characterized by a highly diffuse small-angle curve without any traces of a diffraction maximum. This points to widespread sizes in the phase-separated microregions, incapable of forming an ordered macrolattice.

Despite a low level of small-angle scattering intensity for the acrylate networks, systematic changes of the corresponding profiles with an increase in EGDM content can be followed. In particular, it can be noted that with a crosslink density increase, the small-angle scattering intensity increases over practically the total range of angles which reflects a growing heterogeneity of such networks.

The correlation functions calculated from the experimental small-angle scattering curves for single networks are given in Fig. 3. A considerable difference between the $\gamma(r)$ curve for the PU network and the corresponding curves for the acrylate networks can be noted. The correlation function curves for the acrylate networks display a smoother run to a zero level. This is explained by the fact that the correlation length of nonhomogeneity in the PU network is much shorter than

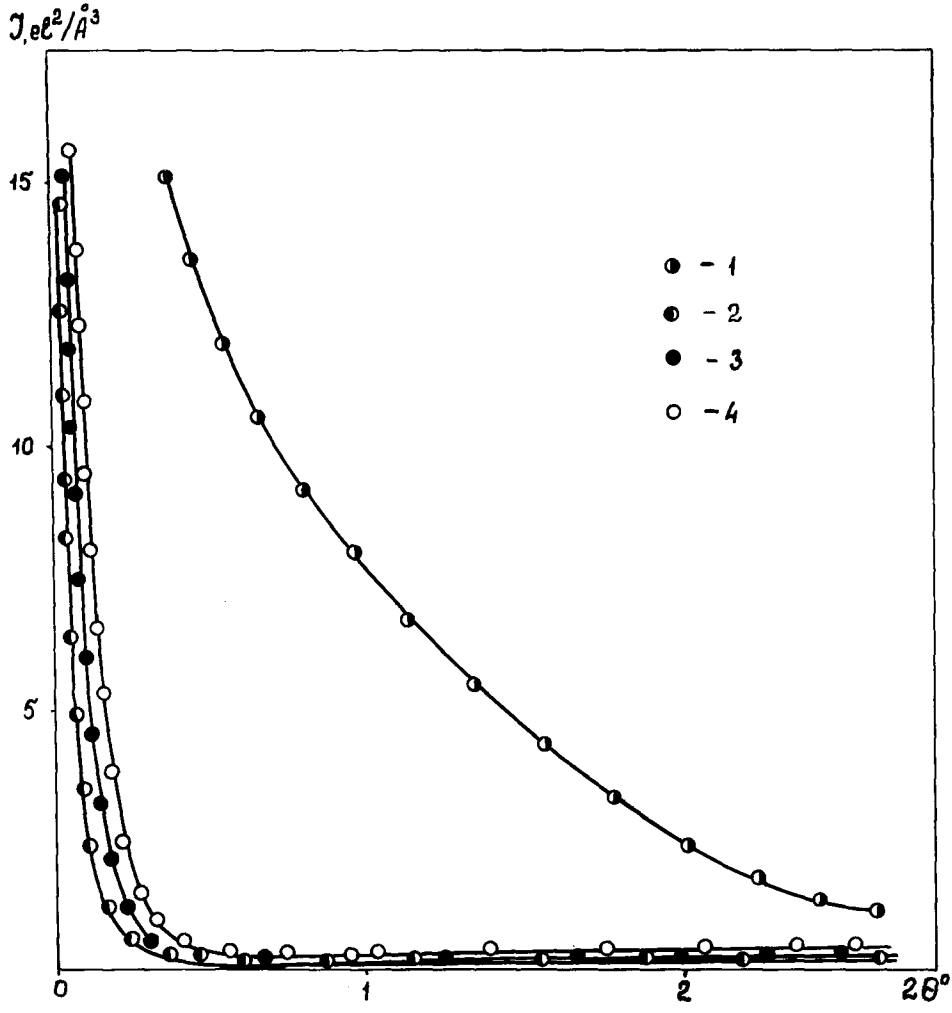

FIG. 2. Small-angle scattering curves for single polymer networks.

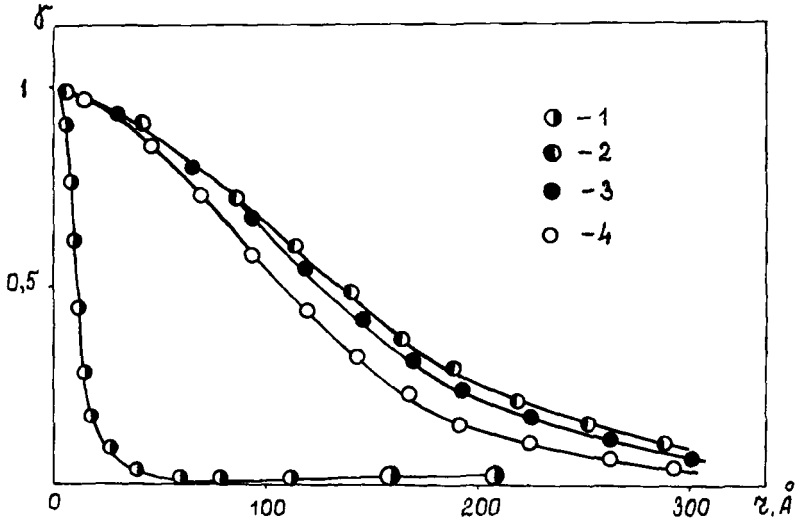

FIG. 3. Correlation functions for single polymer networks.

in the acrylate networks, i.e., the sizes of heterogeneous microregions in block copolyurethane are smaller.

Mean-square electron density fluctuations and average sizes of heterogeneous microregions are summarized in Table 3. These data are in good agreement with qualitative estimates of the sizes of heterogeneous microregions and of the level of heterogeneity based on the small-angle scattering curves and correlation functions. As can be seen, the sizes of microregions in the acrylate networks are almost an order higher than in the PU network. The variations of microregion sizes with EGDM content are of nonmonotonous character, the maximum appearing at a 15% content of this component. The values of mean-square electron density fluctuations are an absolute measure of system turbidity in an x-ray spectrum and characterize the level of heterogeneity as 2 to 3 orders higher for the PU network than for the acrylate networks. Thus, a heterogeneous structure with small microregions of greatly differing electron density is characteristic of the PU network. At the same time, for the acrylate networks, comparatively large heterogeneous microregions and small differences in their electron density are observed.

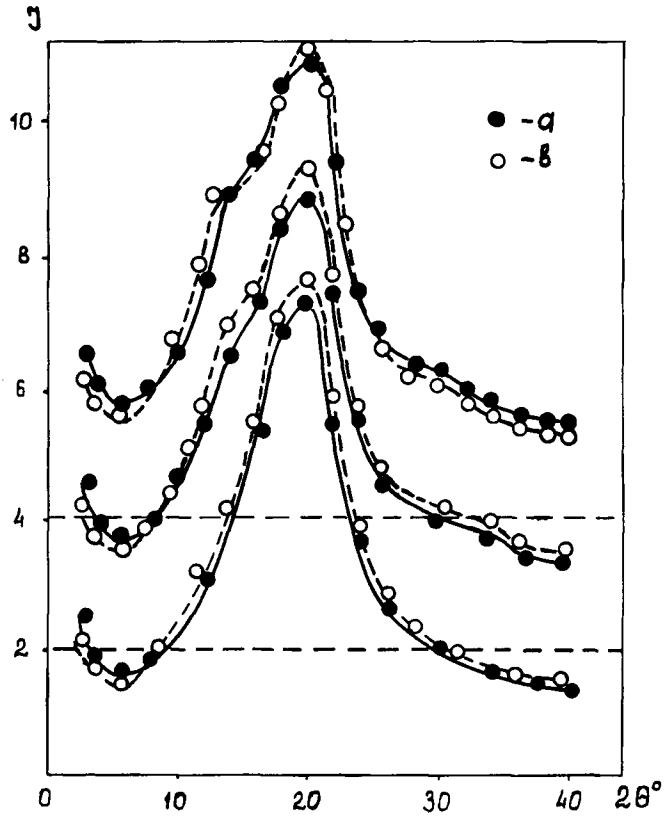

FIG. 4. Wide-angle scattering curves for IPNs: (●) experimental; (○) additive.

TABLE 3. Parameters of Heterogeneous Structure for Single Polymer Networks

Sample no.	D, nm	$\langle\eta^2\rangle$, $e^2 \cdot mol^2 \cdot cm^{-6}$
1	2.4	0.1094×10^{-2}
2	13.3	0.0587×10^{-5}
3	19.9	0.1228×10^{-5}
4	10.9	0.2472×10^{-5}

Interpenetrating Polymer Networks

Wide-angle scattering curves for the IPNs of given compositions are shown in Fig. 4. The dashed lines in this figure correspond to additive curves. It can be seen that IPNs formation does not result in great changes of fine structure as compared to single network components. In particular, IPNs as well as single networks are of liquid-type structure.

To a first approximation, the wide-angle scattering curves for IPNs can be considered as superpositions of scattering curves for single components. First of all, this is confirmed by the maxima appearing on the experimental curves, which are typical of single networks. Comparison of the profiles of experimental and additive curves demonstrates that for IPNs containing the acrylate network with a minimum EGDM content, the contributions from single components to the experimental curve are not as distinct as are those of the additive one. This mainly concerns the first PMMA maximum and the PU maximum. This effect is even more pronounced for IPNs where the penetrating network contains 15% EGDM. The highest additivity is observed for IPNs with a maximum crosslinker content in the penetrating network. The analysis of experimental and additive wide-angle scattering curves for IPNs demonstrates that despite some features of additivity of fine structure in these systems, one can speak about short-range order deviations from additivity, i.e., a certain level of interpenetration of PU and PMMA molecular chains for IPNs is observed. Proceeding from the wide-angle data, one cannot establish which size scales are associated with the interpenetration of network components, but it is quite unambiguous that the level of interpenetration of chains is connected with the crosslink density of the penetrating network. For the densest crosslinked acrylate network (50% EGDM), phase separation is at a maximum level. At lower EGDM contents the relationships become more complex: an increase in EGDM content from 2.5 to 15% does not result in a higher level of phase separation but in a more complete interpenetration of the components. The latter should be considered as a result of the influence of a three-dimensional network of chemical bonds on the interdiffusion of branched fragments of the penetrating network and molecular chains of the matrix one, leading to the retardation of phase separation.

The absence of such an effect at a higher crosslink density of the penetrating network is probably explained by a growing incompatibility of network components.

Small-angle scattering curves for the IPNs of the compositions investigated are given in Fig. 5. The corresponding curves calculated from the additive contributions of single networks to the small-angle scattering of IPNs are also shown in this figure. As can be noted, the level of scattering intensity for IPNs is much higher than that of the theoretical profiles obtained from additive data. At the same time, the profiles of experimental and additive curves near the scattering angles

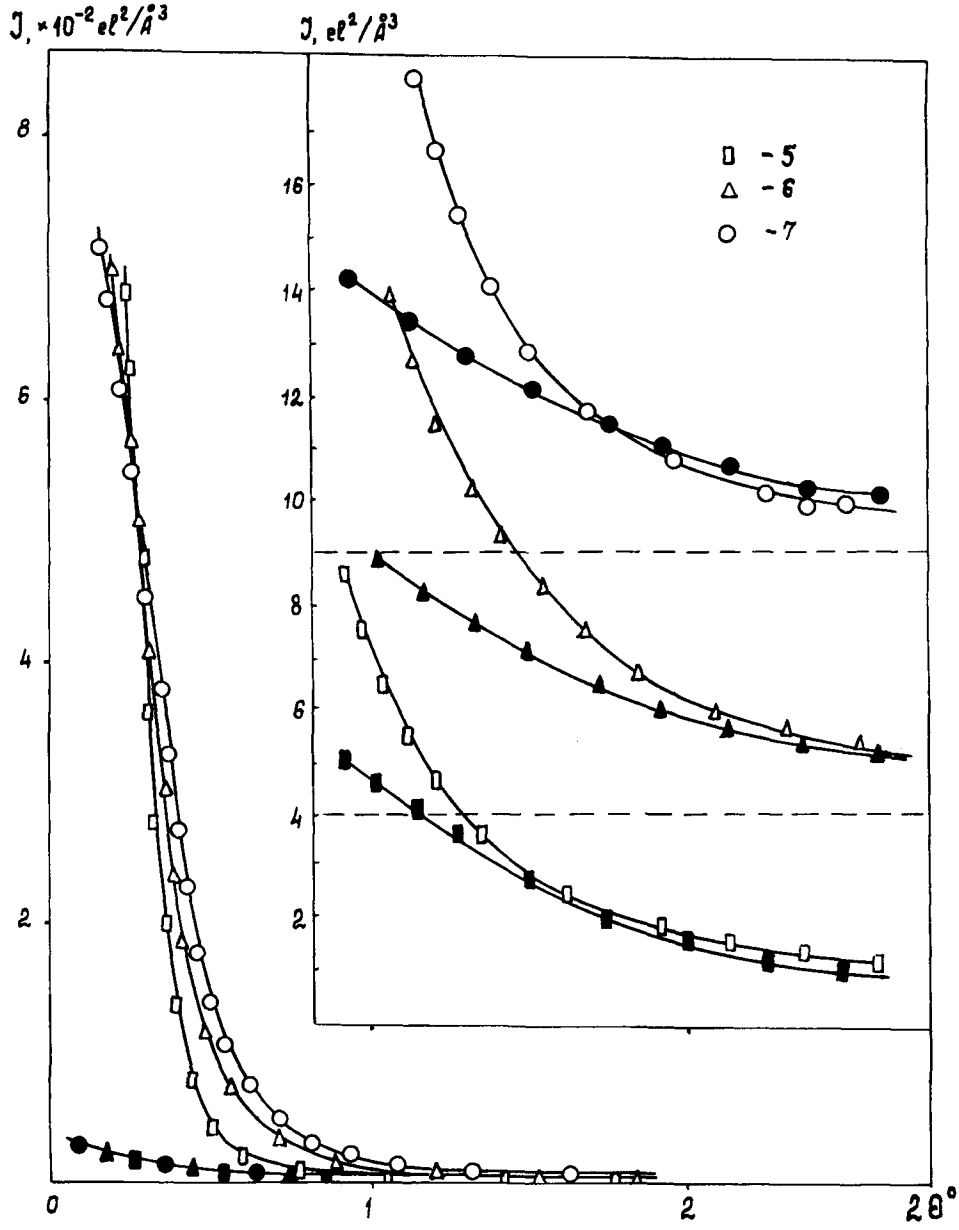

FIG. 5. Small-angle scattering curves for IPNs: open symbols, experimental; filled symbols, additive.

exceeding 2° practically coincide for IPNs with a minimum crosslink density of the acrylate network. The increase of EGDM content in the penetrating network to 15% results in a lower level of scattering intensity for IPNs starting from 2.5° as compared to additive data, this difference increasing as the angle is increased. For IPNs with a maximum EGDM content in the penetrating network, higher additive scattering values as compared to experimental ones become evident starting with 1.5°.

As is known, the scattering intensity of the tails of small-angle curves is determined by the level of density and concentration fluctuations within phase-separated microregions [27]. Therefore, special features of small-angle curves for IPNs should be considered as the result of lower intraphase electron density fluctuations due to a higher crosslink density of the penetrating network, i.e., such fluctuations in IPNs do not become so pronounced compared to single polymer networks. This fact can be explained if we assume that the microphase separation of components during IPNs formation results in microregions with lower electron density fluctuations within the phases due to the partial compatibility of components.

In the range of scattering angles below 1°, the level of scattering intensity for IPNs is very high compared to single components. These differences increase sharply as the angle is decreased. A higher crosslink density of the penetrating network results in a higher level of scattering intensity over the above range of angles. Such effects should be considered as a result of the formation of microregions enriched with one of the components. These conclusions are in good agreement with the wide-angle data presented above.

The correlation curves for IPNs and the corresponding curves obtained by the Fourier transform of additive small-angle scattering curves for these systems are given in Fig. 6. The experimental and additive correlation curves differ greatly, and this points to larger and more segregated heterogeneous microregions in IPNs than in the PU network. Note that the correlation functions for the PU network (Fig. 3) and the additive curves for IPNs are quite similar. This can be explained by the fact that the additive scattering curves for IPNs are similar to those of the PU network. Comparison of the correlation curves for IPNs with different crosslink densities of the penetration network demonstrates that a higher EGDM content in the latter results in a smoother run of correlation functions.

The size distribution curves for heterogeneous microregions calculated from the experimental and additive small-angle scattering curves are given in Fig. 7. Note that with an increase of crosslinker content in the penetrating network, the maximum on these curves is shifted to smaller sizes. At the same time its position remains comparatively near the maxima positions on the distribution functions derived from additive data.

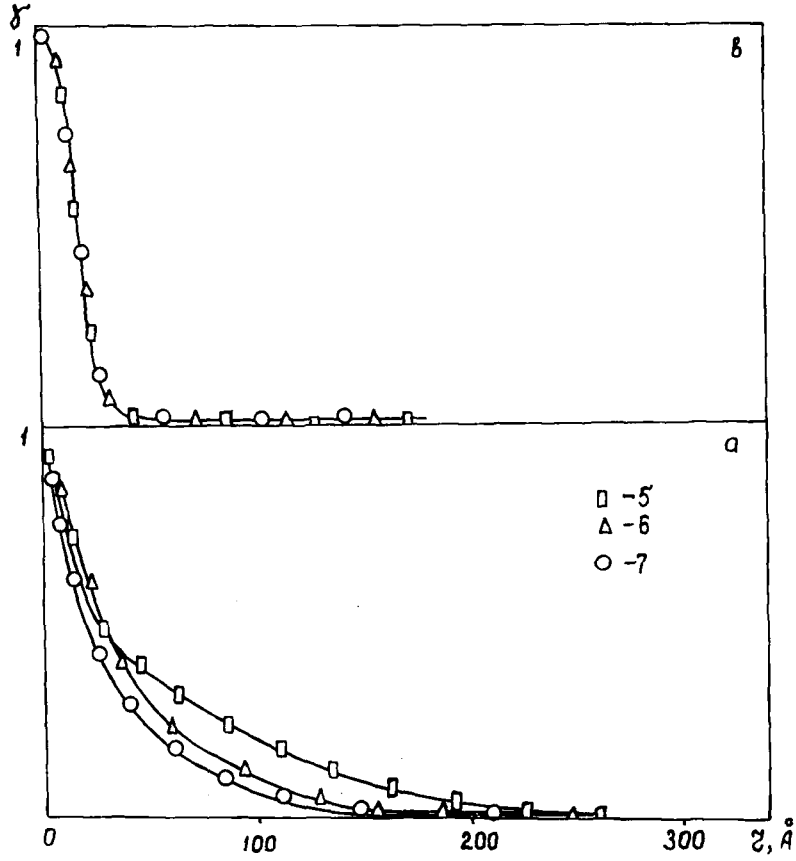

FIG. 6. Correlation functions calculated from experimental (a) and additive (b) small-angle scattering curves for IPNs.

The average sizes of heterogeneous microregions in IPNs calculated from the distribution curves (Fig. 7) and mean-square electron density fluctuations are summarized in Table 4. Note that these average sizes are not large. In this connection it can be concluded that microregions of comparatively large size (tens of nanometers) contributing to the correlation functions are only a small fraction of the total number of phase-separated microregions in IPNs. The latter can obviously be an explanation of the apparent differences in sizes by considering the

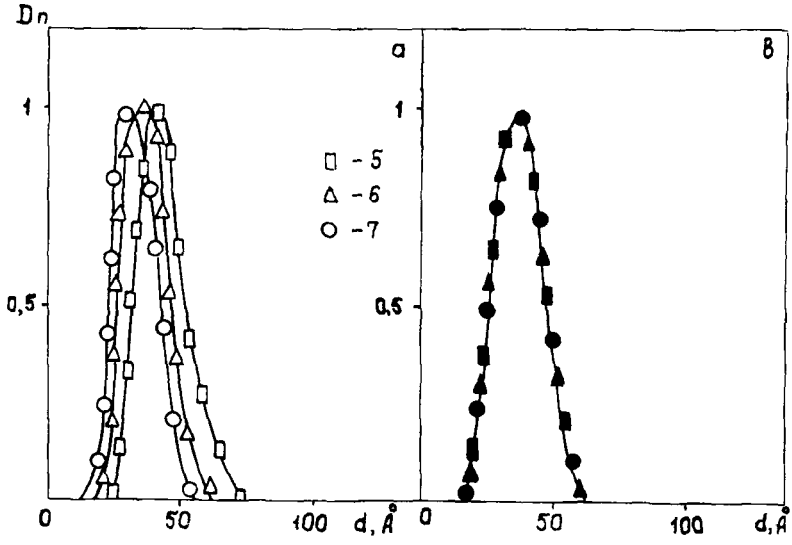

FIG. 7. Size distribution functions for heterogeneous microregions calculated from experimental (a) and additive (b) small-angle scattering curves for IPNs.

correlation functions and size distribution functions for microregions (Figs. 6 and 7). It follows from Table 4 that the variations of average microregion sizes with the growth of EGDM content in the penetrating network are of a nonmonotonous character: at 15% EGDM, microregions of the smallest sizes are formed.

The mean-square electron density fluctuations in IPNs are sometimes higher than the corresponding values for the matrix network. With an increase in the crosslink density of the penetrating network, the $\langle\eta^2\rangle$ values grow monotonically. Since the IPNs structure is complex, this value cannot directly characterize the peculiarities of their microphase structure. To interpret the variations of $\langle\eta^2\rangle$ values

TABLE 4. Parameters of Heterogeneous Structure for IPNs

Sample no.	D, nm	$\langle\eta^2\rangle$, $e^2 \cdot mol^2 \cdot cm^{-6}$	$\overline{\Delta\rho_c^2}$, $e^2 \cdot mol^2 \cdot cm^{-6}$	α	$(\overline{\Delta\rho_c^2})_1$, $e^2 \cdot mol^2 \cdot cm^{-6}$	α_1
5	5.9	0.1455×10^{-2}	0.2329×10^{-2}	0.62	0.1647×10^{-2}	0.88
6	2.9	0.2079×10^{-2}	0.2383×10^{-2}	0.87	0.1701×10^{-2}	1.22
7	4.4	0.2188×10^{-2}	0.2820×10^{-2}	0.78	0.2132×10^{-2}	1.03

with IPNs composition, consider the results of model calculations. In particular, if the comparatively rough approximation that the networks preserve the level of their heterogeneity is used, the theoretical estimation of the mean-square electron density fluctuations can be performed according to

$$\overline{\Delta\rho_c}^2 = (\varphi_1\langle\eta_1^2\rangle + \varphi_2\langle\eta_2^2\rangle) + \varphi_1\varphi_2(\overline{\rho}_1 - \overline{\rho}_2)^2$$
$$= (\overline{\Delta\rho_c}^2)_1 + (\overline{\Delta\rho_c}^2)_2$$

where $\langle\eta_1^2\rangle$ and $\langle\eta_2^2\rangle$ are the mean-square electron density fluctuations for the PU and acrylate networks, $\overline{\rho}_1$ and $\overline{\rho}_2$ are the mean electron densities of the PU and acrylate networks, and φ_1 and φ_2 are the volume fractions of the PU and acrylate networks in IPNs, respectively.

The first and second terms in the above equation determine the contribution to the mean-square electron density fluctuations of IPNs from the heterogeneity of single components and from the heterogeneity associated with the formation of microregions enriched with one of the components. The $\overline{\Delta\rho_c}^2$ and $(\overline{\Delta\rho_c}^2)_1$ values are presented in Table 4. The degree of segregation of the components, α, calculated for the above model as well as the degree of segregation of the components, α_1, for the model, when its heterogeneity is determined only by the heterogeneity of single networks, are also summarized in this table. The latter model is valid for phase separation with the formation of microregions of single networks exceeding 0.1 μm, i.e., the information zone [8, 11] of our small-angle diffractometer. It follows from Table 4 that for the second model the degrees of segregation obtained are quite unreal (exceeding unity). This also confirms the formation of microregions with comparatively small sizes (below tens of nanometers) in IPNs based on single networks. For the first model, degrees of segregation within 0.6–0.9 are obtained, i.e., the compositions of the microregions are very similar to those of single components.

When analyzing the data of Table 4, account should be taken of the approximate character of the model used for the calculation of theoretical values of mean-square electron density fluctuations. The weakest point of this model is the assumption that the supermolecular organization characteristics of single components are preserved in phase-separated microregions. A maximum degree of component segregation for IPNs with 15% EGDM in the penetrating network was apparently obtained due to the incorrectness of the given model. At the same time, the minimum sizes of phase-separated microregions and the greatest deviations of wide-angle data from additive values do not apparently agree with the maximum segregation degree for a given IPN. Taking into account all the above-mentioned points, the degrees of segregation given in Table 4 should be regarded as rough estimates for obtaining a general idea of the comparatively high level of microheterogeneity of the IPNs under study.

One more thing should be mentioned in connection with size distribution curves for heterogeneous microregions calculated by the least-square method [28] and the average sizes of microregions obtained from those curves. These results undoubtedly present an averaged characteristic of heterogeneity in a complex system where phase separation occurs at two levels: at a level of blocks of single components (PU network) and at a level of single components. It appears that in the calculation of size distribution functions, the contribution from small heterogeneous microregions is overestimated. Still, discrimination between the contributions from different heterogeneous microregions can be performed by analyzing the relation between the correlation function logarithm and the radial distance. Then, proceeding from a known relationship [29]:

$$\ln \gamma(r) \approx \exp(-r/l_p)$$

where l_p is the correlation length. From the slope of the corresponding curve, inverse values of the correlation lengths for different scale levels can be found. The results of the corresponding calculations are given in Fig. 8. As can be seen, on the $\ln \gamma(r)$ vs r curves for IPNs with a minimum and average crosslink density, two linear sections can be observed, while on the curves for IPNs with a maximum EGDM content and for the PU network, only one linear section is present. The slope of the curve for the PU network corresponds to a correlation length of about 1.0 nm, and the slope of the initial sections of the IPNs curves corresponds to a correlation length of about 2.0 nm. The slope of the second linear section corresponds to lengths of about 10.0 nm. The slope of the $\ln \gamma(r)$ vs r curve for IPNs with a maximum crosslink density corresponds to l_p of about 4.0–5.0 nm. For the first two IPNs a lower value of correlation length should apparently be associated with nonhomogeneity within PU microregions, while its higher value can be connected when the scale level corresponding to the microregions enriched with one of the components.

Unfortunately, at present there are no available and reliable methods for estimating crosslinking density in IPNs for each constituent network. Therefore, it is impossible to relate microregion size and distribution with network density.

Thus, to summarize the results of wide- and small-angle x-ray analysis of IPNs based on the PU and acrylate networks, it is noted that the microphase structure of these systems is largely determined by the crosslink density of the penetrating networks. The influence of two competing factors on the processes of phase separation is of great importance. On the one hand, a higher crosslink density of the penetrating network contributes to a higher level of separation. On the other hand, the formation of more branched fragments during the copolymerization of methyl methacrylate and EGDM leads to a sharp decrease in the mobility of the

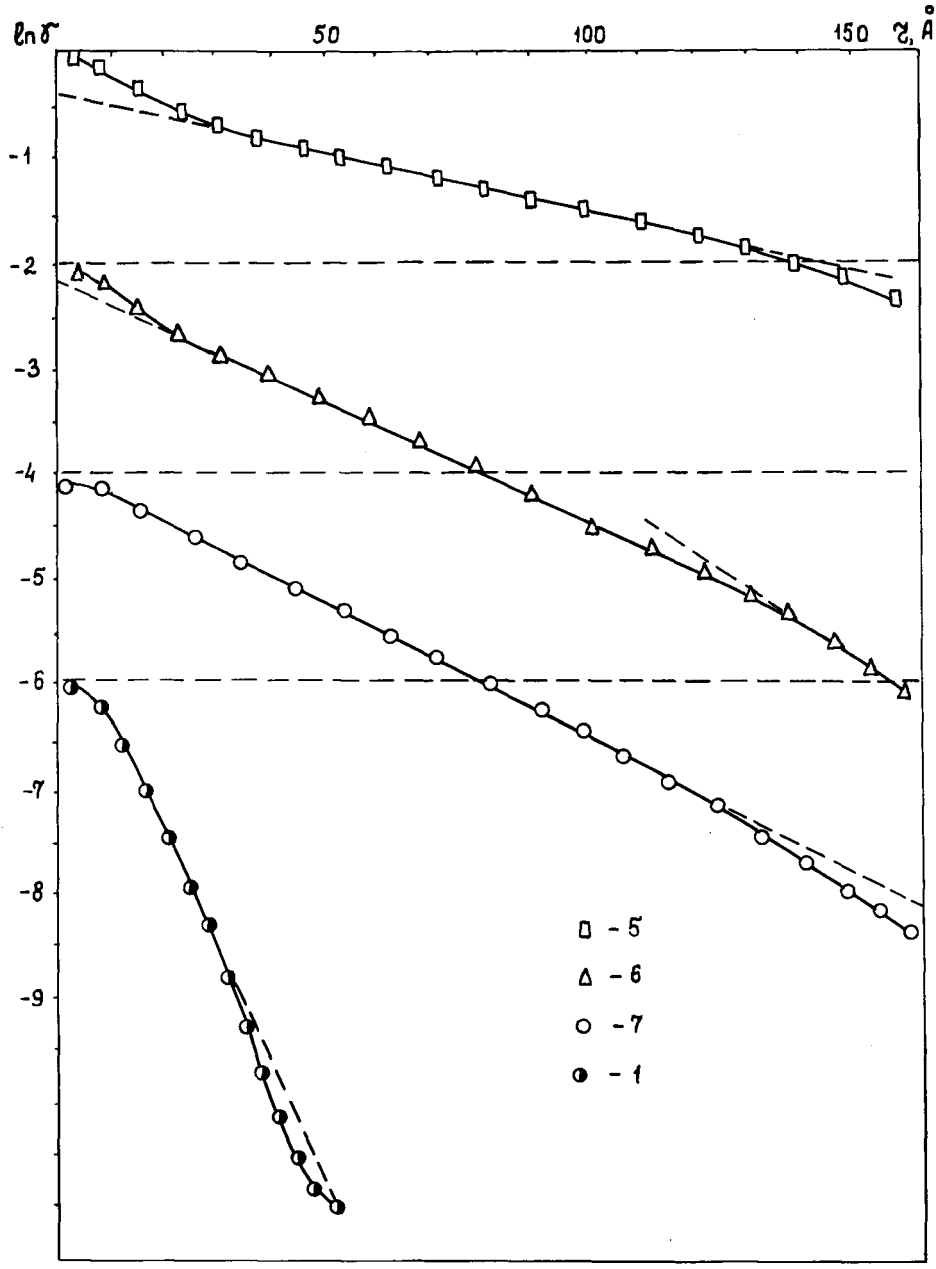

FIG. 8. Plots of ln $\gamma(r)$ vs r. The slopes of linear sections used to calculate correlation lengths are presented as dashed lines.

latter [30] and, therefore, to a greater probability of entanglement of the matrix and the penetrating network fragments. As a result, it appears that at 15% EGDM in the penetrating network, microregions with the greatest interpenetration of both networks are formed.

REFERENCES

[1] Yu. S. Lipatov and L. M. Sergeeva, *Interpenetrating Polymer Networks,* Naukova Dumka, Kiev, 1975.
[2] L. H. Sperling, *Interpenetrating Polymer Networks and Related Materials,* Plenum, New York, 1981.
[3] Yu. S. Lipatov and L. M. Sergeeva, *Usp. Khim., 45,* 138 (1976).
[4] Yu. S. Lipatov, *Mech. Compos. Mater.,* p. 771 (1983) (in Russian).
[5] Yu. S. Lipatov and V. V. Shilov, *Kompoz. Polim. Mater., 11,* 55 (1981).
[6] Yu. S. Lipatov and V. V. Shilov, *Usp. Khim., 53,* 1197 (1984).
[7] A. Morin, H. Djomo, and G. C. Meyer, *Polym. Eng. Sci., 23,* 394 (1983).
[8] D. Klempner, *Angew. Chem., Int. Ed. Engl., 17,* 97 (1978).
[9] M. Akay, S. N. Rollins, and E. Riordan, *Polymer, 29,* 37 (1988).
[10] S. C. Kim, D. Klempner, K. C. Frisch, W. Radigan, and H. L. Frisch, *Macromolecules, 9,* 263 (1976).
[11] S. C. Kim, D. Klempner, K. C. Frisch, and H. L. Frisch, *Ibid., 10,* 1187 (1976).
[12] G. Allen, M. J. Bowden, D. J. Blundell, F. G. Hutchinson, G. M. Jeffs, and J. Vyvoda, *Polymer, 14,* 597 (1973).
[13] G. Allen, M. J. Bowden, G. Lewis, D. J. Blundell, and G. M. Jeffs, *Ibid., 15,* 13 (1974).
[14] D. J. Blundell, G. W. Longman, G. D. Wignall, and M. J. Bowden, *Ibid., 15,* 33 (1974).
[15] H. Djomo, A. Morin, M. Damyanidu, and G. C. Meyer, *Ibid., 24,* 65 (1983).
[16] S. R. Jin, J. M. Widmaier, and G. C. Meyer, *Ibid., 29,* 346 (1988).
[17] Yu. Lipatov, L. Karabanova, L. Sergeeva, L. Gorbach, and S. Skiba, *Vysokomol. Soedin, Ser. B., 29*(4), 274 (1986).
[18] C. Mai and G. P. Johari, *J. Polym. Sci., Part B, Polym. Phys., 25,* 1903 (1987).
[19] R. W. Hertzberg and J. A. Manson, *Fatigue in Engineering Plastics,* Academic, New York, 1980.
[20] O. Kratky, *Z. Elektrochem., 58,* 49 (1954).
[21] Yu. S. Lipatov, V. V. Shilov, Yu. P. Gomza, and N. E. Kruglyak, *X-Ray Methods of Investigation of Polymeric Systems,* Naukova Dumka, Kiev, 1982.

[22] O. Kratky, I. Pils, and B. I. Shmidt, *J. Colloid Interface Sci., 21,* 24 (1966).
[23] C. G. Vonk, *FFSAXS Program for the Processing of Small-Angle X-Ray Scattering Data,* DSM, Geleen, 1975.
[24] J. Hosemann and S. N. Bagchi, *Direct Analysis of Diffraction by Matter,* North-Holland, Amsterdam, 1962.
[25] Yu. S. Lipatov, V. V. Shilov, and Yu. P. Gomza, *Dokl. Akad. Nauk USSR, 61* (1982).
[26] R. Bonart and E. H. Muller, *J. Macromol. Sci.—Phys., B10,* 345 (1974).
[27] J. Rathje and W. Ruland, *Colloid Polym. Sci., 254,* 358 (1976).
[28] C. G. Vonk, *J. Appl. Crystallogr., 9,* 433 (1976).
[29] A. Guinier and G. Fournet, *Small-Angle Scattering of X-Rays,* Wiley, New York, 1955.
[30] K. Huber, W. Burchard, and L. I. Fetters, *Macromolecules, 17,* 541 (1984).

Received July 2, 1988
Revision received July 31, 1989